Code Development on Fission Product Behavior under Severe Accident –Validation of Aerosol Sedimentation

Kwang Soon Ha*, Sung Il Kim, Jin-Sung Jang, and Dong Ha Kim
Korea Atomic Energy Research Institute, 1045 Daedeok-daero, Yuseong-gu, Daejeon, Korea
**Corresponding author: tomo@kaeri.re.kr*

1. Introduction

The major threat of nuclear power plants to the safety of the public comes from the radioactive material present in the reactor vessel. The amount of radionuclides released into the containment or to the environment is always the focus of the design, operation, and regulation of nuclear power plants. In particular, the large amount of radioactive materials might be released if a core melt accident, that is, a severe accident, occurs in a nuclear power plant. Therefore, it is very important to estimate the behaviors of radioactive materials under severe accident conditions.

The transport phases of the radioactive materials can be divided into gas and aerosol. The gas and aerosol phases of the radioactive materials move through the reactor coolant systems and containments as loaded on the carrier gas or liquid, such as steam or water. Most radioactive materials might escape in the form of aerosols from a nuclear power plant during a severe reactor accident [1], and it is very important to predict the behavior of these radioactive aerosols in the reactor cooling system and in the containment building under severe accident conditions. Aerosols are designated as very small solid particles or liquid droplets suspended in a gas phase. The suspended solid or liquid particles typically have a range of sizes of 0.01 μm to 20 μm. Aerosol concentrations in reactor accident analyses are typically less than 100 g/m^3 and usually less than 1 g/m^3. At these concentrations, the aerosol particles have little effect on the gas hydrodynamics, but the gas dynamics profoundly affect the behavior of the suspended particles. The behaviors of the larger aerosol particles are usually described through continuum mechanics. The smallest particles have diameters less than the mean free path of the gas phase molecules, and the behavior of these particles can often be described well by free molecular physics. The vast majority of aerosol particles arising in reactor accident analyses have behaviors in the very complicated intermediate regime between the continuum mechanics and free molecular limit. In this regime, the aerosol behavior must be described using some approximate solution of the Boltzmann equation [1]. When there are continuing sources of aerosol to the gas phase or when there are complicated processes involving engineered safety features, much more complicated size distributions develop. It is not uncommon for aerosols in reactor containments to have bimodal size distributions for at least some significant periods of time early during an accident. Salient features of aerosol physics under reactor accident conditions that will affect the nature of the aerosols are (1) the formation of aerosol particles, (2) growth of aerosol particles, (3) shape of aerosol particles, (4) deposition of particles on the surfaces, and (5) a re-suspension of aerosol particles [1].

At KAERI, a fission product module has been developed to predict the behaviors of the radioactive materials in the reactor coolant system under severe accident conditions. The fission product module consists of an estimation of the initial inventories, species release from the core, aerosol generation, gas transport, and aerosol transport. The final outcomes of the fission product module designate the radioactive gas and aerosol distribution in the reactor coolant system. The aerosol sedimentation models in the fission product module were validated using ABCOVE and LACE experiments.

2. Descriptions of FP module

As shown in Fig. 1, the fission product module consists of an estimation of the initial inventories, species release from the core, aerosol generation, gas transport, and aerosol transport.

In the fission product module, the initial inventories of the fission species in UO_2 such as Xe, Kr, Cs, I, Ba, Sr, Te, Sb, Mo, Ru, Zr (fission), Sn, and La are calculated based on SANDIA-ORIGEN calculation data [2], which are function of rector thermal power and the fuel cycle. SANDIA-ORIGEN calculation data were obtained by assuming a 3412 MWt Westinghouse PWR, end-of-cycle equilibrium core, and three-region core, each initially loaded with fuel enriched to 3.3% U-235, with a constant specific power density of 38.3 MW per metric ton of U, a three-year refueling cycle, an 80% capacity factor, and three regions having burn-ups of 11,000, 22,000, and 33,000 MWd per metric ton of uranium [2]. The other inventories that come from the structure materials, such as Zr, Fe, Cr, Ni, and Mn, are calculated from the masses of the cladding, stainless steel, and Inconel alloy.

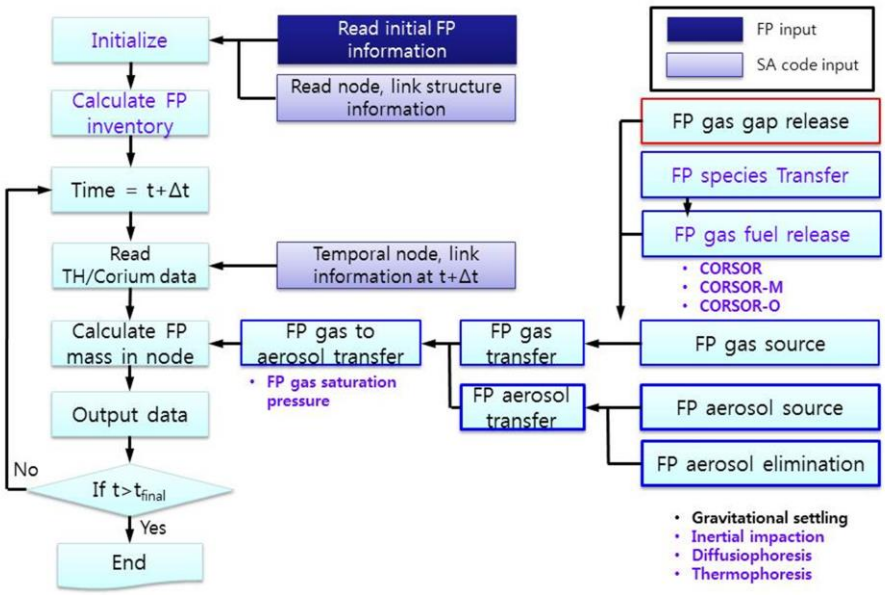

Fig. 1. Structure of fission product module

Radioactive and nonradioactive species may be released from the core, cladding, structural materials such as stainless steel, and Inconel alloy if the materials heat up. The species release rates are calculated using the CORSOR model [2], which is a function of the material temperature. The released species are 8 classified groups that have similar chemical properties, that is, noble gases, alkali metal iodides, alkali metal hydroxides, chalcogens, alkaline earths, paltinoids, rare earths, and structural materials, as shown in Table I. It is assumed that the released species from the core, classing, and structural materials are initially formed as representative groups of the gas phases. Each group has its own saturation gas pressure according to the temperature. Therefore, some amount of aerosols of each group may be generated if the gas pressure is higher than the saturation pressure, and some aerosols of each group may be evaporated into gas if the gas pressure is lower than the saturation pressure. The saturation pressure of group 1, noble gases, is zero, and therefore, the noble gases cannot form aerosols.

The gases and aerosols of fission products are transported through the reactor coolant systems and containments as loaded into the carrier gas or liquid such as steam or water. If the reactor coolant systems and containments are nodalized and linked by a general thermal-hydraulic code, the fission product transport equations for the gas and aerosol phases of the *i*-group can be designated by equations (1) and (2) at the given thermal-hydraulic node *n*.

$$\frac{dm_{v,i}^n}{dt} = \dot{m}_{v,i,in}^n - \dot{m}_{v,i,out}^n + \dot{G}_{v,i}^n \qquad (1)$$

$$\frac{dm_{a,i}^n}{dt} = \dot{m}_{a,i,in}^n - \dot{m}_{a,i,out}^n - \lambda_{t,i}^n m_{a,i}^n + \dot{G}_{a,i}^n \qquad (2)$$

Table I: Fission Product Groups

Group	Representative	Species member
1. Noble gases	Xe	Xe, Kr
2. Alkali metal iodides	CsI	CsI
3. Alkali metal hydroxides	CsOH	CsOH
4. Chalcogens	Te	Te, Sb
5. Alkaline earths	Ba	Ba, Sr
6. Platinoids	Ru	Ru, Mo
7. Rare earths	La	La, Zr(fission)
8. Structural materials	Zr	Zr, Fe, Cr, Ni, Mn

The *i*-group gas generation rate in a node *n*, $\dot{G}_{v,i}^n$, in equation (1) can be obtained by the CORSOR model [2] or user input data. The *i*-group aerosol generation rate in node *n*, $\dot{G}_{a,i}^n$, in equation (2) can be obtained by the user input. The *i*-group gas and aerosol mass flow rates in node *n* are estimated using the mass transport rates of the carrier gas or liquid, which are calculated by the thermal-hydraulic module in the severe accident codes. Therefore, the fission product model should be coupled with the thermal-hydraulic module. In equation (2), the *i*-group aerosol removal coefficient in a node *n*, $\lambda_{t,i}^n$, can be obtained by considering the aerosol behaviors such as the gravitational settling, thermophoresis, impaction, diffusiophoresis (steam condensation), vapor

condensation, and vapor revolatilization. There are several approaches to predict the aerosol dynamics such as a sectional method [2, 3] and mass tracking method [4, 5, 6, 7]. Based on the mass tracking method similar to the MAAP 5 code [7], some aerosol behaviors such as the gravitational settling [4], impaction [4], diffusiophoresis [5], and thermophoresis [6] are considered to estimate the aerosol removal coefficient. The gas and aerosol transport equations in equations (1) and (2) are discretized to apply semi-implicit (Gauss-Jordan elimination) or explicit (Runge-Kutta-Fehlberg, RK45) numerical schemes for time marching.

After solving the *i*-group gas and aerosol transport equations, the *i*-group gas and aerosol masses are re-evaluated using the saturation pressure of the *i*-group gas according to the temperature, as mentioned before.

The fission product module has been prepared using C++ language. A user can select a semi-implicit or explicit numerical scheme for solving the gas and aerosol transport equations, and add user-defined gas and aerosol groups, which include the properties and source rates.

3. Results and Discussion

The aerosol coagulation and removal models in the developed fission product module were verified through a comparison with the MELCOR results [2] in the ABCOVE (AB-5, AB-6, AB-7) and LACE (LA2) experiments. In all calculations, thermal-hydraulic data obtained by MELCOR calculations were used to calculate the airborne mass by the fission product module. User-defined aerosol groups in each calculation were created to match with the experimental conditions. Only the aerosol sedimentation model during each calculation was activated in the fission product module.

3.1 ABCOVE Experiments

The purpose of the ABCOVE program was to provide a basis for judging the adequacy of aerosol behavior codes in describing the inherent aerosol attenuation in containment buildings during postulated accidents. For the ABCOVE experiments, a large test vessel was used with a diameter of 7.62 m, height of 20.3 m, and volume of 852 m^3 [8].

In AB-5 [8], sodium aerosol with a mass mean diameter of 1.5 μm and standard deviation of 1.8 was used to simulate the aerosol behavior under high concentration conditions. The sodium aerosol was injected at an injection rate of 0.455kg/s during 14 to 885 seconds into the vessel, and the airborne aerosol concentration was measured. For the calculation, the aerosol collision shape factor and dynamic shape factor were set by 2.25 and 1.5. Figure 2 shows the calculation results on the AB-5 experimental conditions. As shown in Fig. 2, The temporal airborne sodium aerosol mass agreed excellently with the MELCOR results.

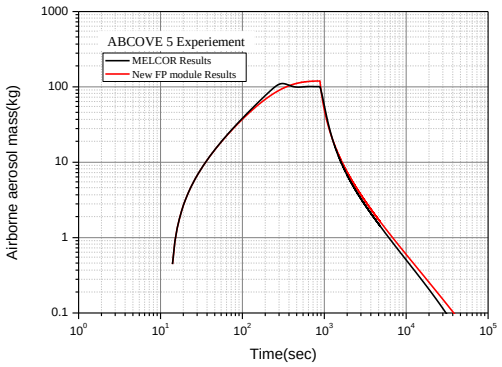

Fig. 2. Temporal variation of airborne aerosol mass compared with MELCOR results on AB-5 experiment

In AB-6 [8], two types of aerosols were injected into the test vessel. NaI aerosol with a mass mean diameter of 0.544 μm and standard deviation of 1.55, and NaOx aerosol with a mass mean diameter of 0.5 μm and standard deviation of 2.0 were used to simulate the aerosol behavior. NaI aerosol was injected at an injection rate of 0.00014kg/sec during 0 to 3000 seconds, and NaOx aerosol was injected at an injection rate of 0.00014kg/sec during 620 to 5000 seconds into the large vessel, and the airborne aerosol concentration was measured. For the calculation, aerosol collision shape factors and dynamic shape factors for NaI and NaOx were set equally to 2.25 and 1.5. Figure 3 shows the calculation results on the AB-6 experimental conditions. The temporal airborne NaOx aerosol mass agreed excellently with the MELCOR results. However, the temporal airborne NaI aerosol mass by the fission product module was decayed more slowly compared with the MELCOR results. This may be due to the aerosol model discrepancy. That is, the MELCOR code is applied to the sectional method, which can trace aerosol size variations; however, the current fission product module simply considered the total aerosol mass.

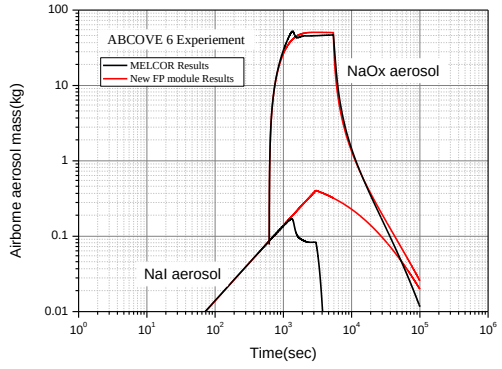

Fig. 3. Temporal variations of airborne aerosol masses compared with the MELCOR results on the AB-6 experiment

In AB-7 [8], which was similar to AB-6, two types of aerosols were injected into the test vessel. NaI aerosol with a mass mean diameter of 0.54 μm and standard deviation of 1.55, and NaOH aerosol with a mass mean diameter of 0.5 μm and standard deviation of 2.0, were used to simulate aerosol behavior. NaOH aerosol was injected at an injection rate of 0.00503kg/s during 0 to 600 seconds, and NaI aerosol was injected with an injection rate of 0.000197kg/s during 600 to 2400 seconds into the test vessel, and the airborne aerosol concentration was measured. For the calculation, the aerosol collision shape factors and dynamic shape factors for NaI and NaOH were set equally to 2.25 and 1.5. Figure 4 shows the calculation results under the AB-7 experimental conditions. The temporal airborne NaOH and NaI aerosol masses during the injection periods agreed excellently with the MELCOR results. However, the temporal airborne NaOH and NaI aerosol masses during the decay periods had some discrepancies between the results by the current fission product module and by MELCOR. This may be due to aerosol model differences, that is, the aerosol size and mass tracking.

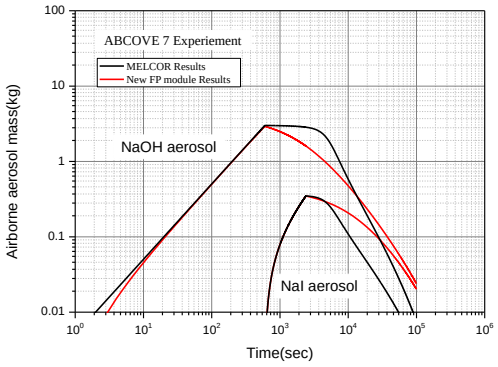

Fig. 4. Temporal variations of airborne aerosol masses compared with MELCOR results on AB-7 experiment

3.2 LACE Experiments

The objectives of the LACE program were to investigate experimentally the inherent aerosol retention behavior for postulated, high-consequence accident situations, and to provide a database for validating the containment aerosol and related thermal-hydraulic computer codes [8]. Two nonradioactive aerosols, representative of severe accident conditions, were included in test LA2. Cesium hydroxide (CsOH) was used as a water-soluble species, and manganese oxide (MnO) was used as an insoluble species. An LA-2 test was conducted in four consecutive thermal-hydraulic stages, as shown below. Period 1 (-30 to 0 min) was a rapid heat-up phase in which steam was injected upward along the vessel centerline from a point in the lower part of the vessel. Heated nitrogen was added through the aerosol delivery line at a low rate. Period 2 (0 to 50.2 min) was the aerosol release period during which aerosols, steam, and noncondensible gases were added to the containment system through the aerosol delivery line. Steam was also added at a reduced rate through the vertical steam pipe in the lower part of the test vessel. Period 3 (50.2 to 1,000 min) was a slow cool-down period in which steam and nitrogen were added to the containment at a reduced rate through the vertical steam pipe and aerosol delivery pipe, respectively. The upper and lower leak paths were closed at 396 minutes. Period 4 (1000 to 2,895 min) was a cool-down period in which nitrogen addition continued at a low rate through the aerosol delivery line but steam injection was discontinued. Figure 5 shows the calculation results under the LA-2 experimental conditions. The temporal airborne CsOH and MnO aerosol masses during the injection periods agreed excellently with the MELCOR results. However, the temporal airborne CsOH and MnO aerosol masses during the decay periods had some discrepancies between the results by the current fission product module and by MELCOR. In the LA-2 experiment, some steam was ejected into the test vessel, and thus steam was condensed on the aerosol particles. Because there is no steam condensation model in the current fission product module, CsOH and MnO aerosol masses decreased more slowly compared with the MELCOR results.

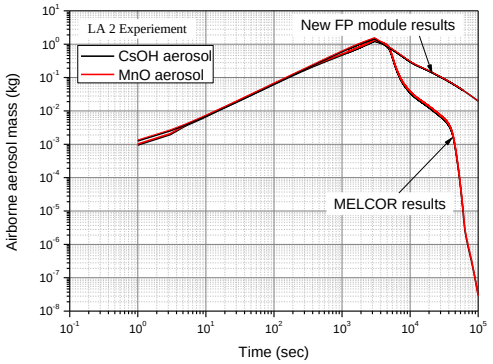

Fig. 5. Temporal variations of airborne aerosol masses compared with MELCOR results on LA-2 experiment

3. Conclusions

A fission product module has been developed to predict behaviors of the radioactive materials in the reactor coolant system under severe accident conditions. The fission product module consisted of an estimation of the initial inventories, species release from the core, aerosol generation, gas transport, and aerosol transport. The final outcomes of the fission product module designate the radioactive gas and aerosol distribution in the reactor coolant system. The aerosol sedimentation models in the fission product module were validated using ABCOVE and LACE experiments. There were

some discrepancies on the predicted aerosol decay masses between the developed fission product module and MELCOR code. These discrepancies come from model differences of the aerosol sedimentation and steam condensation.

The fission product module will be updated on the species release from the gap between the fuel and cladding, decay heat evaluation, aerosol size tracking, etc.

NOMENCLATURE

$m_{v,i}^{n}$ *i*-group gas mass in *n* node
$\dot{m}_{v,i,in}^{n}$ *i*-group gas mass inflow rate into *n* node
$\dot{m}_{v,i,out}^{n}$ *i*-group gas mass outflow rate from *n* node

$\dot{G}_{v,i}^{n}$ *i*-group gas mass source rate in *n* node
$m_{a,i}^{n}$ *i*-group aerosol mass in *n* node
$\dot{m}_{a,i,in}^{n}$ *i*-group aerosol mass inflow rate into *n* node
$\dot{m}_{a,i,out}^{n}$ *i*-group aerosol mass outflow rate from *n* node
$\dot{G}_{a,i}^{n}$ *i*-group aerosol mass source rate in *n* node
$\lambda_{t,i}^{n}$ *i*-group aerosol removal coefficient in *n* node

ACKNOWLEDGMENTS

This work was supported by the Nuclear and Development of the Korea Institute of Energy Technology Evaluation and Planning (KETEP) grant funded by the Korea government (Ministry of Trade, Industry, and Energy) (No. 20141510101670).

REFERENCES

[1] State-of-the-art report on nuclear aerosols, NEA/CSNI/ R(2009)5, Nuclear Energy Agency, Committee on the safety of nuclear installations, Dec. 17, 2009.
[2] R.O. Gauntt, R.K. Cole, C.M. Erickson, R.G. Gido, R.D. Gasser, S.B. Rodriguez, and M.F. Young, MELCOR Computer Code Manual, Vol. 2: Reference Manuals, Version 1.8.5 May 2000, Decay Heat(DCH) Package Manual, RadioNuclide(RN) Package Reference Manual, NUREG/CR-6119, Vol. 2, Rev. 2, SAND2000-2417/2, October 2000.
[3] F. Gelbard, MAEROS User Manual, SAND80-0822, NUREG/CR-1391, December 1982.
[4] Michael Epstein and Phillip G. Ellison, "Correlations of the rate of removal of coagulating and depositing aerosols for application to nuclear reactor safety problems," NED, 107, p. 327-344, 1988.
[5] R. T. Lahey and F. J. Moody, The thermal-hydraulics of a boiling water nuclear reactor. 2nd ed., ANS, La Grange Park, 1993.
[6] Michael Epstein and Phillip G. Ellison, "Thermophoretic deposition of particles in nature convection flow from a vertical plate," J. Heat Transfer, Vol. 107, p.272-276, 1985
[7] MAAP5 Code Manual
[8] Francisco J. Souto, F. Eric Haskin, Lubomyra N. Kmetyk, MELCOR 1.8.2 assessment: aerosol experiments ABOVE AB5, AB6, AB7, and LACE LA2, SAND-2166, SNL. 1994.